Journal of Neurochemistry
Lippincott Williams & Wilkins, Philadelphia

Molecular Cloning and Regional Distribution of a Human Proton Receptor Subunit with Biphasic Functional Properties

Kazimierz Babinski, Khanh-Tuoc Lê, and Philippe Séguéla

Cell Biology of Excitable Tissue Group, Montreal Neurological Institute, McGill University, Montreal, Quebec, Canada

Abstract: Small changes of extracellular pH activate depolarizing inward currents in most nociceptive neurons. It has been recently proposed that acid sensitivity of sensory as well as central neurons is mediated by a family of proton-gated cation channels structurally related to *Caenorhabditis elegans* degenerins and mammalian epithelial sodium channels. We describe here the molecular cloning of a novel human proton receptor, hASIC3, a 531-amino acid-long subunit homologous to rat DRASIC. Expression of homomeric hASIC3 channels in *Xenopus* oocytes generated biphasic inward currents elicited at pH <5, providing the first functional evidence of a human proton-gated ion channel. Contrary to the DRASIC current phenotype, the fast desensitizing early component and the slow sustained late component differed both by their cationic selectivity and by their response to the antagonist amiloride, but not by their pH sensitivity (pH_{50} = 3.66 vs. 3.82). Using RT-PCR and mRNA blot hybridization, we detected hASIC3 mRNA in sensory ganglia, brain, and many internal tissues including lung and testis, so hASIC3 gene expression was not restricted to peripheral sensory neurons. These functional and anatomical data strongly suggest that hASIC3 plays a major role in persistent proton-induced currents occurring in physiological and pathological conditions of pH changes, likely through a tissue-specific heteropolymerization with other members of the proton-gated channel family. **Key Words:** Proton-gated channel—Degenerin—Amiloride—Trigeminal sensory neurons—Pain—*Xenopus* oocytes.
J. Neurochem. **72,** 51–57 (1999).

Acid sensing is a specific kind of chemoreception that plays a critical role in the detection of nociceptive pH imbalances occurring in conditions of cramps, trauma, inflammation, and hypoxia (Lindahl, 1974). In mammals, a population of small-diameter primary sensory neurons in the dorsal root ganglia and trigeminal ganglia express specialized pH-sensitive surface receptors activated by increase of extracellular proton concentration (Bevan and Yeats, 1991). Native electrophysiological responses of sensory neurons to applications of pH 5.8–6.5 are characterized by a fast desensitizing inward current followed by a slow sustained current (Krishtal and Pidoplichko, 1981). Clarifying the native molecular composition of proton sensors in human sensory neurons will be an important step in the rational development of a novel class of analgesics. A family of genes coding for neuronal proton-gated channels subunits has been discovered recently (Garcia-Anoveros et al., 1997; Waldmann et al., 1997*a*,*b*). Heterologously expressed amiloride-sensitive homomeric rat acid-sensing ion channel (ASIC) (Waldmann et al., 1997*b*) responds to small pH changes by a fast desensitizing sodium-selective current, whereas mammalian degenerin 1 (MDEG1) (Waldmann et al., 1996) and dorsal root ganglia ASIC (DRASIC) (Waldmann et al., 1997*a*) require drastic pH changes to gate desensitizing and biphasic currents, respectively. ASIC and MDEG1 can associate together to generate a heteromeric channel activated at low pH (<5) with unique kinetics and ionic selectivities (Bassilana et al., 1997). A neuronal splicing variant of MDEG1 was shown to modulate DRASIC biophysical properties by heteromeric association (Lingueglia et al., 1997). These proton-gated channels share a putative two-transmembrane domain topology and colocalization in small-diameter capsaicin-sensitive sensory neurons with P2X ATP-gated channels (North, 1997). From their sequence, they belong to an expanding gene superfamily including mammalian epithelial sodium channels (Canessa et al., 1994*a*,*b*), pickpocket (PPK) and ripped pocket (RPK) subunits from *Drosophila* (Adams et al., 1998), degenerins of *Caenorhabditis elegans* (Corey and Garcia-Anoveros, 1996), and the FMRFamide-gated channel of *Helix aspersa* (Lingueglia et al., 1995). Despite their potential importance in monitoring pH changes in CNS and sensory pathways, human proton receptor genes have not yet been functionally characterized. We report here for the first time the heterologous expression of a human proton-gated channel, as well as significant interspecies differences observed both in functional properties and in regional distribution of acid sensors.

Received May 22, 1998; revised manuscript received August 3, 1998; accepted August 6, 1998.

Address correspondence and reprint requests to Dr. P. Séguéla at Montreal Neurological Institute, 3801 University, Rm. 778, Montreal, Quebec, Canada H3A 2B4.

Abbreviations used: ASIC, acid-sensing ion channel; DRASIC, dorsal root ganglia ASIC; MDEG1, mammalian degenerin 1.

MATERIALS AND METHODS

Molecular cloning

Using the tblastn algorithm, virtual screening of the dbEST database of NCBI (Lennon et al., 1996) with probes corresponding to the protein motif LXFPAVTLCNXNXXRXS, conserved in all known members of the degenerin/ENaC/ASIC family, led to the identification of human EST sequences encoding a novel member of the proton sensor gene family (GenBank accession nos. AA449579 and AA429417). The clone tagged by 5′ EST AA449579 and by 3′ EST AA449322 from a total fetus cDNA library was sequenced on both strands, using walking primers and an ALF DNA sequencer (Pharmacia-LKB). Full-length hASIC3 was subcloned directionally into unique *Eco*RI and *Not*I sites of eukaryotic vector pcDNA3 (Invitrogen) for cytomegalovirus promoter-driven heterologous expression in *Xenopus* oocytes.

Electrophysiology in *Xenopus* oocytes

Oocytes surgically removed from adult *Xenopus laevis* were treated for 2 h at room temperature with type II collagenase (GibcoBRL) in Barth's solution under constant agitation. Selected oocytes at stage IV–V were defolliculated manually before nuclear microinjections (Bertrand et al., 1991) of 5 ng of hASIC3 in pcDNA3 vector. After 2–4 days of expression at 19°C in Barth's solution containing 50 μg/ml gentamicin, currents were recorded in the two-electrode voltage-clamp configuration, using an OC-725B amplifier (Warner Instruments). Whole-cell currents were acquired and digitized at 500 Hz on a Macintosh IIci computer with an A/D NB-MIO16XL interface (National Instruments), then recorded traces were postfiltered at 100 Hz in an Axograph (Axon Instruments). Agonist, amiloride, and wash solutions were prepared in a modified Ringer's solution containing 115 m*M* NaCl, 2.5 m*M* KCl, and 1.8 m*M* $CaCl_2$ in 5–20 m*M* HEPES (Sigma) buffer adjusted with NaOH or HCl at pH 2–8 and applied on oocytes by constant perfusion (10–12 ml/min) at room temperature. Mean ± SEM values corresponded to measurements from a minimum of five oocytes.

RT-PCR and mRNA dot-blot hybridization

Total RNA from postmortem samples of normal human trigeminal ganglia were isolated by using TriZOL reagent (GibcoBRL), then 1 μg was subjected to random-primed reverse transcription using Superscript (GibcoBRL). Around 100 ng of RT-cDNA was used as template for PCR with Expand DNA polymerase (Boehringer-Mannheim). Specific hASIC3 primers TCAGTGGCCACCTTCCTCTA (forward) and ACAGTCCAGCAGCATGTCATC (reverse) were used to amplify the region corresponding to nucleotides 175–513 (see Fig. 1A). After initial template denaturation for 2 min at 94°C, thermal cycles consisted of 45 s at 94°C, 45 s at 55°C, and 2 min at 72°C for 30 cycles. Molecular identity and homogeneity of PCR products were checked by sizing and specific restriction patterns. Initial sample loading was checked by coamplification of glyceraldehyde-3-phosphate dehydrogenase housekeeping mRNA. RNA samples not subjected to reverse transcription but PCR-amplified in identical conditions provided our negative controls.

Known amounts of human poly(A)$^+$ RNA (89–514 ng), isolated from various fetal and adult normal tissues and normalized for the transcription levels of several housekeeping genes (Clontech), were dot-blotted and probed with the ^{32}P-labeled *Eco*RI–*Xba*I fragment of hASIC3 cDNA at high stringency (final elution at 65°C in 0.3 × saline–sodium citrate buffer for 10 min). After exposure for 16 h, hybridization signals were acquired and quantitated by using a Storm phosphorimager (Molecular Dynamics), and then analyzed in densitometry with ImageQuant software (Molecular Dynamics).

Data analysis

All data are expressed as mean ± SEM values and represent results of experiments done in triplicate on at least three separate oocyte preparations. Statistical methods consisted of two-tailed *t* tests and regression analysis available with the PRISM software package (GraphPad, San Diego, CA, U.S.A.). Nonlinear regression on *I/V* curves used the Boltzman equation, whereas dose–response curves were fitted with the four-parameter logistic equation. Multiple comparison of sigmoidal curves was evaluated by the partial *F* test, using ALLFIT software (De Léan et al., 1978).

RESULTS

Primary structure of hASIC3 channel subunit

Sequence analysis of the 1.7-kb-long hASIC3 poly(A)$^+$ mRNA revealed an open reading frame encoding 531 amino acids (Fig. 1A), with initiation of translation at the proximal Met codon located at nucleotide position 22. The predicted molecular mass of 59 kDa for the immature protein was confirmed by in vitro translation (data not shown). According to the current topological model based on primary structure analysis and biochemical tests, a large domain of 365 amino acids faces the extracellular side of the plasma membrane (Canessa et al., 1994*a*,*b*). In this extracellular domain, a total of 15 cysteine residues are highly conserved in the ASIC family, with the exception of Cys^{267} being absent in human BNaC1 (hASIC2) only. Two potential sites for Asn-linked glycosylation, Asn^{175} and Asn^{398}, are located in this cysteine-rich loop. Consensus sites for phosphorylation by casein kinase II (Ser^{5}) and by protein kinase C (Ser^{39}, Ser^{478}, Ser^{493}, and Ser^{521}) are found in the intracellular N-terminal domain of hASIC3 as well as in the intracellular C-terminal domain (Fig. 1A). The hASIC3 subunit displays 83% of identity with rat DRASIC subunit at the amino acid level, 48% with human BNaC2 (hASIC1) and 47% with BNaC1 (hASIC2) (Fig. 1B). Therefore, hASIC3 belongs to the proton-gated channel family, itself a branch of the degenerin/ENaC/FMRFamide-gated channel phylogenetic tree (Fig. 1C).

Functional and pharmacological properties of homomeric hASIC3 channels

When heterologously expressed in *Xenopus* oocytes, hASIC3 subunits assemble into functional homomeric channels activated by low extracellular pH (Fig. 2A). Rapid changes of extracellular pH (Fig. 2B and C) revealed a biphasic response. This unique phenotype was characterized by a fast and rapidly desensitizing current followed by a slow and sustained current that returned to baseline only on return to physiological pH. The relative amplitude of the fast current appeared dependent on the slope of the pH gradient applied (Fig. 2A and C). However, we found the pH sensitivity of the two hASIC3-mediated currents to be almost identical with a pH_{50} of

A

```
TCGCACGACGCGGTTCTGGCCATGAAGCCCACCTCAGGCCCAGAGGAGGCCCGGCGGCAGCCCTCGGACATCCGC     75
                    M  K  P  T  (S) G  P  E  E  A  R  R  Q  P  S  D  I  R       18
GTGTTCGCCAGCAACTGCTCGATGCACGGGCTGGGCCACGTCTTCGGGCCAGGCAGCCTGAGCCTGCGCCGGGGG    150
V  F  A  S  N  C  S  M  H  G  L  G  H  V  F  G  P  G  S  L  (S) L  R  R  [G]    43
ATGTGGGCAGCGGCCGTGGTCCTGTCAGTGGCCACCTTCCTCTACCAGGTGGCTGAGAGGGTGCGCTACTACAGG     225
M  W  A  A  A  V  V  L  S  V  A  T  F  L  Y  Q  V  A  E  R  V  R  Y  Y  R       68
GAGTTCCACCACCAGACTGCCCTGGATGAGCGAGAAAGCCACCGGCTCGTCTTCCCGGCTGTCACCCTGTGCAAC     300
E  F  H  H  Q  T  A  L  D  E  R  E  S  H  R  L  V  F  P  A  V  T  L  C  N       93
ATCAACCCACTGCGCCGCTCGCGCCTAACGCCCAACGACCTGCACTGGGCTGGGTCTGCGCTGCTGGGCCTGGAT     375
I  N  P  L  R  R  S  R  L  T  P  N  D  L  H  W  A  G  S  A  L  L  G  L  D       118
CCCGCAGAGCACGCCGCCTTCCTGCGCGCCCTGGGCCGGCCCCCTGCACCGCCCGGCTTCATGCCCAGTCCCACC     450
P  A  E  H  A  A  F  L  R  A  L  G  R  P  P  A  P  P  G  F  M  P  S  P  T       143
TTTGACATGGCGCAACTCTATGCCCGTGCTGGGCACTCCCTGGATGACATGCTGCTGGACTGTCGCTTCCGTGGC     525
F  D  M  A  Q  L  Y  A  R  A  G  H  S  L  D  D  M  L  L  D  C  R  F  R  G       168
CAACCTTGTGGGCCTGAGAACTTCACCACGATCTTCACCCGGATGGGAAAGTGCTACACATTTAACTCTGGCGCT     600
Q  P  C  G  P  E  [N] F  T  T  I  F  T  R  M  G  K  C  Y  T  F  N  S  G  A       193
GATGGGGCAGAGCTGCTCACCACTACTAGGGGTGGCATGGGCAATGGGCTGGACATCATGCTGGACGTGCAGCAG     675
D  G  A  E  L  L  T  T  T  R  G  G  M  G  N  G  L  D  I  M  L  D  V  Q  Q       218
GAGGAATATCTACCTGTGTGGAGGGACAATGAGGAGACCCCGTTTGAGGTGGGGATCCGAGTGCAGATCCACAGC     750
E  E  Y  L  P  V  W  R  D  N  E  E  T  P  F  E  V  G  I  R  V  Q  I  H  S       243
CAGGAGGAGCCGCCCATCATCGATCAGCTGGGCTTGGGGGTGTCCCCGGGCTACCAGACCTTTGTTTCTTGCCAG     825
Q  E  E  P  P  I  I  D  Q  L  G  L  G  V  S  P  G  Y  Q  T  F  V  S  C  Q       268
CAGCAGCAGCTGAGCTTCCTGCCACCGCCCTGGGGCGATTGCAGTTCAGCATCTCTGAACCCCAACTATGAGCCA     900
Q  Q  Q  L  S  F  L  P  P  P  W  G  D  C  S  S  A  S  L  N  P  N  Y  E  P       293
GAGCCCTCTGATCCCCTAGGCTCCCCCAGCCCCAGCCCCAGCCCTCCCTATACCCTTATGGGGTGTCGCCTGGCC     975
E  P  S  D  P  L  G  S  P  S  P  S  P  S  P  P  Y  T  L  M  G  C  R  L  A       318
TGCGAAACCCGCTACGTGGCTCGGAAGTGCGGCTGCCGAATGGTGTACATGCCAGGCGACGTGCCAGTGTGCAGC    1050
C  E  T  R  Y  V  A  R  K  C  G  C  R  M  V  Y  M  P  G  D  V  P  V  C  S       343
CCCCAGCAGTACAAGAACTGTGCCCACCCGGCCATAGATGCCATCCTTCGCAAGGACTCGTGCGCCTGCCCCAAC    1125
P  Q  Q  Y  K  N  C  A  H  P  A  I  D  A  I  L  R  K  D  S  C  A  C  P  N       368
CCGTGCGCCAGCACGCGCTACGCCAAGGAGCTCTCCATGGTGCGGATCCCGAGCCGCGCCGCCGCGCGCTTCCTG    1200
P  C  A  S  T  R  Y  A  K  E  L  S  M  V  R  I  P  S  R  A  A  A  R  F  L       393
GCCCGGAAGCTCAACCGCAGCGAGGCCTACATCGCGGAGAACGTGCTGGCCCTGGACATCTTCTTTGAGGCCCTC    1275
A  R  K  L  [N] R  S  E  A  Y  I  A  E  N  V  L  A  L  D  I  F  F  E  A  L       418
AACTATGAGACCGTGGAGCAGAAGAAGGCCTATGAGATGTCAGAGCTGCTTGGTGACATTGGGGGCCAGATGGGC    1350
N  Y  E  T  V  E  Q  K  K  [A  Y  E  M  S  E  L  L  G  D  I  G  G  Q  M  G]    443
CTTTTCATCGGGGCCAGCCTGCTCACCATCCTCGAGATCCTAGACTACCTCTGTGAGGTGTTCCGAGACAAGGTC    1425
L  F  I  G  A  S  L  L  T  I  L  E  I  L  D  Y  L  C  E  V  F  R  D  K  V       468
CTGGGATATTTCTGGAACCGACAGCACTCCCAAAGGCACTCCAGCACCAATCTGCTTCAGGAAGGGCTGGGCAGC    1500
L  G  Y  F  W  N  R  Q  H  (S) Q  R  H  S  S  T  N  L  L  Q  E  G  L  G  (S)    493
CATCGAACCCAAGTTCCCCACCTCAGCCTGGGCCCCAGACCTCCCACCCCTCCCTGTGCCGTCACCAAGACTCTC    1575
H  R  T  Q  V  P  H  L  S  L  G  P  R  P  P  T  P  P  C  A  V  T  K  T  L       518
TCCGCCTCCCACCGCACCTGCTACCTTGTCACACAGCTCTAGACCTGCTGTCTGTGTCCTCGGAGCCCCGCCCTG    1650
S  A  (S) H  R  T  C  Y  L  V  T  Q  L  .                                       531
ACATCCTGGACATGCCTAGCCTGCACGTAGCTTTTCCGTCTTCACCCCAAATAAAGTCCTAATGCATCAAAAAAA    1725
AAAAAAA                                                                         1732
```

B

	hASIC2	hASIC1	α	β	γ	δ
hASIC3	47.9	46.6	17.3	15.4	16.6	14.9
hASIC2		64.5	15.2	17.2	16.4	15.0
hASIC1			13.1	17.0	16.9	15.0
α				26.7	29.1	33.4
β					31.4	22.6
γ						21.8

C

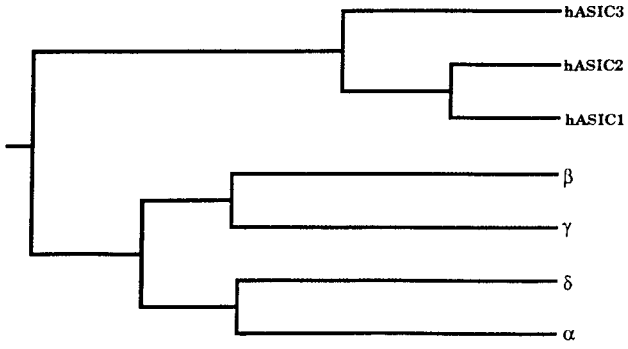

FIG. 1. Nucleotide and predicted amino acid sequence of hASIC3 cDNA (**A**), deposited in GenBank database under the accession no. AF057711. Two stretches of 20–34 amino acids corresponding to potential transmembrane domains, identified in Kyte–Doolittle hydrophobicity plot, are highlighted. Consensus phosphorylation sites in intracellular domains and *N*-glycosylation sites in extracellular domain are indicated by circled and boxed residues, respectively. Homology (%) of hASIC3 (**B**) and phylogenetic relationships (**C**) with known members of the human ASIC/ENaC family. The protein dendrogram was generated by using UPGMA algorithm (Geneworks 2.5.1, Oxford Molecular Group).

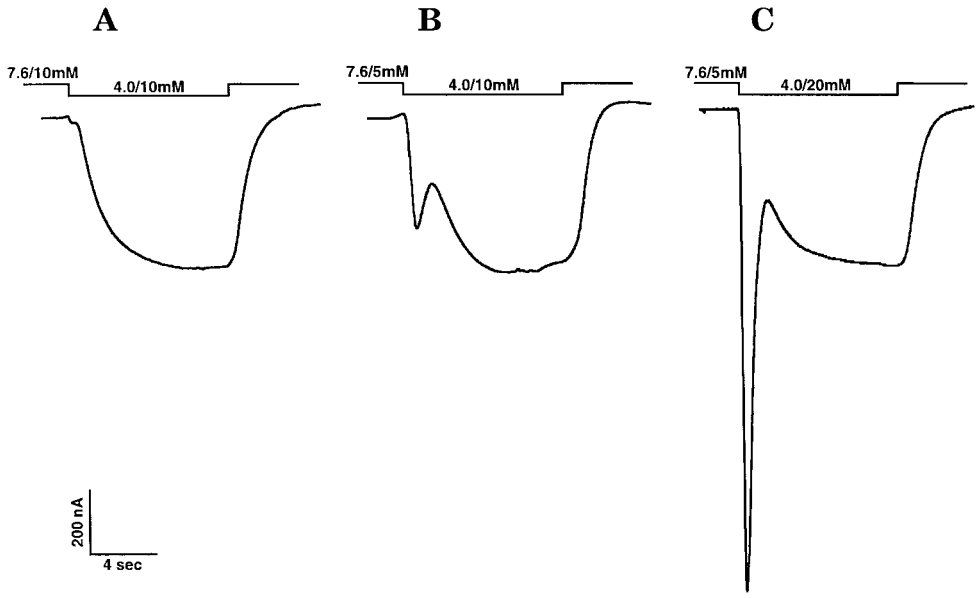

FIG. 2. Biphasic current phenotype of homomeric hASIC3 channels; effects of increasing rates of pH change. Oocytes were clamped at −70 mV and continuously perfused with Ringer's buffer containing 10 m*M* HEPES at pH 7.6. pH was then dropped to 4.0 for 10 s with increasing pH gradients obtained by raising the buffer capacity differential between control and test buffers: **A:** pH 7.6–4.0 in 10 m*M* HEPES. **B:** pH 7.6 in 5 m*M* to pH 4.0 in 10 m*M* HEPES. **C:** pH 7.6 in 5 m*M* to pH 4.0 in 20 m*M* HEPES. Controls done with the test buffers at pH 7.6 did not activate the hASIC3 channel. Oocytes injected with injection buffer alone showed no inward currents. The amplitude of the early but not the late component, and thus the ratio of early to late peak currents, appears to be very sensitive to the speed at which the pH drops from normal to acid pH values.

3.66 ± 0.06 (fast) vs. 3.82 ± 0.04 (slow) (Fig. 3). The positive cooperativity reflected in the dose–response curve profile, n_{Hfast} = 1.57 ± 0.3 and n_{Hslow} = 1.55 ± 0.17, indicated that at least two protonations on two subunits are required to gate the cation channel. To study possible differences of ionic selectivity between fast and slow components, we performed a current–voltage relationship at pH 4.0 in normal Ringer. The peak amplitude of the fast component displayed some voltage dependence from its slight inward rectification, whereas the slow and sustained component was ohmic in the range from −70 to + 70 mV (Fig. 4B). Furthermore, although both reversal potentials were greater than 30 mV as expected for channels conducting mainly sodium, we measured a ΔE_{rev} = +15 ± 3.2 mV ($p < 0.01$) between the fast (+32.9 ± 4.4 mV) and the slow component (+48.2 ± 4.8 mV) (Fig. 4A and B). These two phases of proton-induced hASIC3 current differed also by their sensitivity to the antagonist amiloride. Coapplication of 100 μM amiloride with pH 4.0 under conditions of biphasic response demonstrated a more efficient blockade of the fast (62.8 ± 6.5%) than of the slow current (28.7 ± 4.6%) by amiloride (Fig. 5A and B).

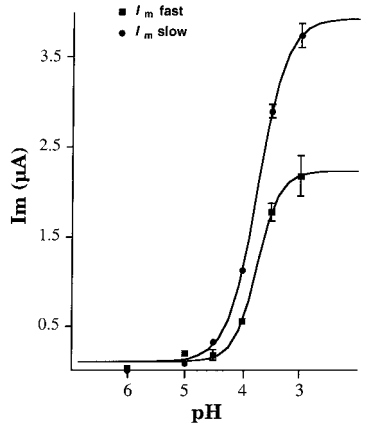

FIG. 3. Dose–response curves of pH activation of hASIC3 currents. Dose–response curves were constructed in 20 m*M* HEPES buffered at different pH values from 6.0 to 3.0. Peak currents of fast and slow currents were analyzed with the four-parameter logistic equation and the partial *F* test for statistical comparison. Each point represents mean ± SEM from this typical experiment. Apart from the maximal response, no other significant difference was observed between both curves.

Central and peripheral distribution of hASIC3 gene expression

As a rough index of anatomical distribution and mRNA abundance, we noticed several cDNAs encoding hASIC3 in total fetus and testis cDNA libraries represented in the dbEST database. Results obtained in RNA hybridization at high stringency confirmed that the hASIC3 gene is transcribed in a wide spectrum of internal organs as well as in the CNS (Fig. 6). In the adult stage, hASIC3 transcripts were detected in lung, lymph nodes, kidney, pituitary, heart, and testis as well as in brain and spinal cord. A developmental up-regulation of hASIC3 gene expression was apparent when comparing fetal vs. adult mRNA levels in lung and kidney (Fig. 6).

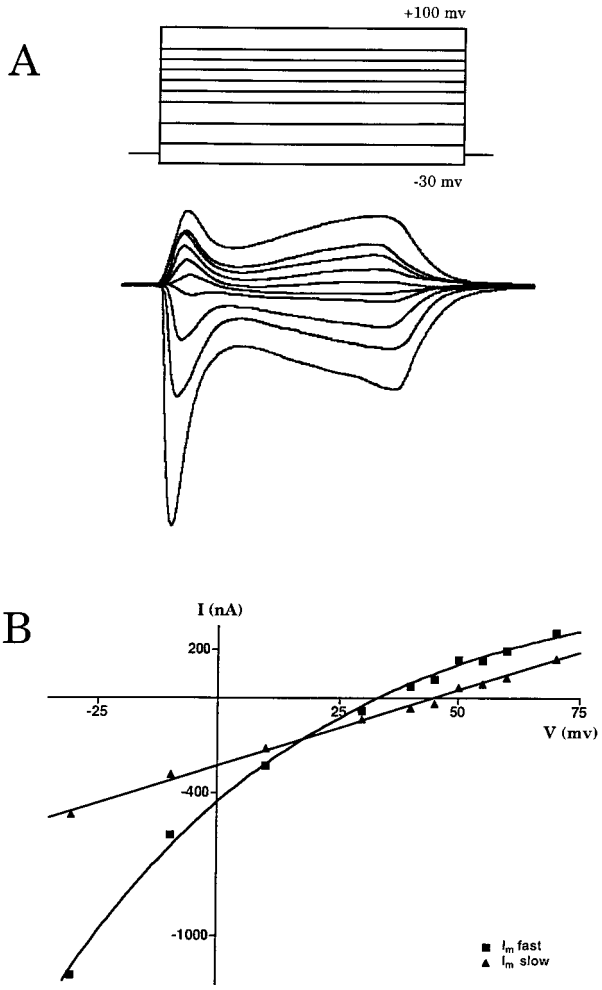

FIG. 4. Current–voltage (*I/V*) relationship of the fast and slow hASIC3 currents. Recordings were done in Ringer's buffer containing (m*M*) NaCl 115, KCl 2.5, $CaCl_2$ 1.8, and HEPES 5, pH 7.6. The *I/V* relationship was established by measuring peak currents of both fast and slow responses to pH 4.0 (applied 1 s after voltage step) at different membrane potentials, after subtracting background currents recorded without pH applications (**A**). Peak current values were plotted (**B**) and reversal potential estimated from linear (slow current) and nonlinear (fast current) regression analysis. A and B represent a typical experiment where reversal potentials were 33.4 and 44.8 mV, respectively, for the fast and slow currents.

Thus, hASIC3 subunit expression is not restricted exclusively to sensory ganglia as is its rat homologue DRASIC, explaining our decision to use a chronological nomenclature that is distribution independent. The potentially important function of noninactivating proton-gated channels in nociceptive sensory neurons was nevertheless confirmed by the detection of high levels of ASIC3 mRNA in adult human trigeminal ganglia, using RT-PCR (Fig. 7).

DISCUSSION

We report in the present study the characterization of a novel central member of the human degenerin/ENaC channel family, genetically identical to hTNaC isolated from human testis (Ishibashi and Marumo, 1998). Significant homologies found both in extracellular and in transmembrane domains of the predicted hASIC3 subunit with known proton-gated channels were substantiated by our electrophysiological data showing activation of the homomeric channel by changes of extracellular pH. In contrast to rat ASIC, which responds to slight external acidification, a drastic pH decrease (pH_{50} ~4) was required to activate hASIC3 channels when heterologously expressed in *Xenopus* oocytes.

Despite a strong conservation of primary structure, the hASIC3 channel displayed several interesting differences of properties with its rodent homologue DRASIC. Two potential regulatory protein kinase C sites found in hASIC3 sequence are conserved in DRASIC (Ser^{39} and Ser^{521}), so the functional impact of phosphorylation of these domains will be worth investigating in the context of heterologous sensitization of nociceptive response by

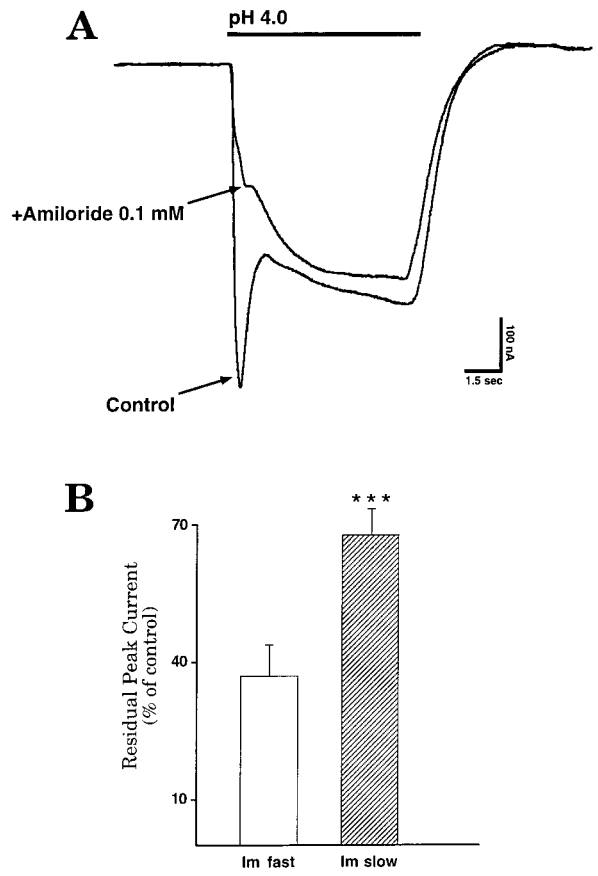

FIG. 5. Differential sensitivity of the fast and slow hASIC3 currents to amiloride. hASIC3 currents were activated by pH 4.0 in the presence and absence of 100 μM amiloride (**A**). Inhibition by amiloride was much stronger on the fast than the sustained current. **B:** Data are mean ± SEM values (n = 17) of residual peak currents during amiloride application for the fast (37.2 ± 6.4%) and sustained (72.0 ± 3.8%) components expressed as percentages of controls. Statistical significance was evaluated by unpaired two-tailed *t* test (***$p < 0.001$).

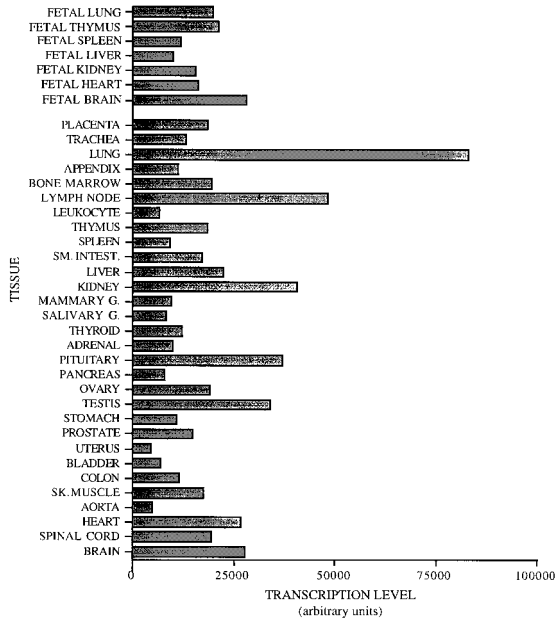

FIG. 6. Distribution of hASIC3 mRNA in normal human tissues. High-stringency hybridization of radiolabeled hASIC3 cDNA on human poly(A)$^+$ RNA isolated from brain, spinal cord, and internal tissues as well as from week 17–28 fetal tissues was quantitated by densitometric analysis in phosphorimaging. Amounts of poly(A)$^+$ RNA target were normalized across tissues to allow direct comparisons of transcription levels (see Materials and Methods).

metabotropic receptors linked to phospholipase C (Dray and Perkins, 1993). Both rat and human channels generated biphasic responses in the homomeric form, but the human proton sensor required lower pH (pH_{50} = 3.66 vs. 6.9) for the activation of the early fast component (Waldmann et al., 1997*a*). The difference of reversal potentials that we detected between desensitizing and sustained currents of hASIC3 reflected a measurable change in ionic selectivity between these two states of activation, not observed in the case of DRASIC (Waldmann et al., 1997*a*). Nevertheless, reversal potentials in the +30 to +50 mV range were consistent with the activity of cation channels mainly conducting sodium ions. One of the pharmacological features of channels belonging to the ASIC/ENaC family is their sensitivity to blockade by the antidiuretic amiloride and its derivatives (Kleyman and Cragoe, 1988). Coapplication of amiloride with low pH inhibited more the early than the late response. Both hASIC3 currents, however, were sensitive to the antagonist, a situation different from what has been reported with DRASIC where the sustained current was instead potentiated by amiloride (Waldmann et al., 1997*a*).

Species differences were also striking when analyzing the anatomical distribution of hASIC3 gene expression. Whereas rat DRASIC was reported to be transcribed exclusively in dorsal root ganglia (Waldmann et al., 1997*a*), we noticed moderate to high levels of hASIC3 gene expression in many peripheral tissues as well as in brain, spinal cord, and sensory ganglia, using dot-blot RNA hybridization and RT-PCR amplification. In contrast, Ishibashi and Marumo (1998) reported the exclusive expression of hASIC3 in testis from northern blot data. This discrepancy could be explained by differences in detection sensitivity, in differences of normalization of mRNA according to housekeeping genes, or by the fact that our methods of detection did not distinguish alternative splicing variants of the hASIC3 gene. From our data on the expression of hASIC3 in lung and testis, two tissues with high levels of transcription and low density of innervation, we infer that acid-sensing functions mediated by proton-gated channels are more anatomically extended than previously expected. Alternatively, the hASIC3 subunit could be a component of mechano-gated (Tavernarakis et al., 1997) or ligand-gated cation channels (Lingueglia et al., 1995) not yet characterized. It is worth noticing that the cerebellum, where hASIC1 (BNaC2) and hASIC2 (BNaC1) mRNAs are expressed at high levels, is one of the central regions with the highest density of hASIC3 mRNA. Like other known ionotropic receptors, ASIC channels most likely assemble in heteromeric complexes. It has been reported that the three different ENaC subunits coassemble into tetrameric (Firsov et al., 1998) or nonameric (Snyder et al., 1998) channels and that homomeric FMRFamide-gated channels are tetramers (Coscoy et al., 1998). Therefore, proton-gated hASIC3 channel subunits could associate with hASIC1 and/or hASIC2 in multimeric channels of unknown stoichiometry in central and peripheral neurons.

The molecular composition of surface sensors mediating the biphasic pH response recorded in most small-diameter capsaicin-sensitive sensory neurons remains to be clarified. We propose that hASIC3 subunits, by a functional dominant effect, provide the slow kinetics leading to a sustained pH-induced current. However, the native pH response is likely generated by the activities of at least two different channels, for the following reasons: (1) The two currents differ by their ionic selectivity; the early phase is sodium selective (pK/pNa = 0.14) and the late phase is nonselective for small cations (pK/pNa

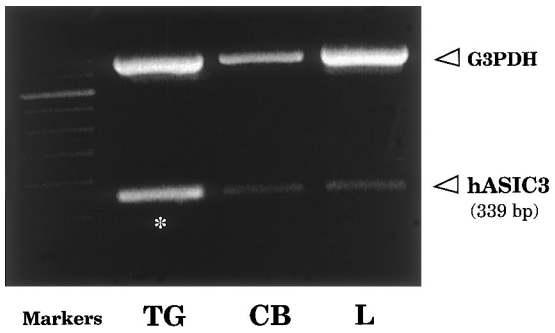

FIG. 7. High levels of transcription of hASIC3 gene in sensory ganglia enriched in nociceptive neurons. Localization of hASIC3 and reporter glyceraldehyde-3-phosphate dehydrogenase (G3PDH) mRNAs in human trigeminal ganglia (TG), cerebellum (CB), and lung (L), using RT-PCR amplification with specific exact match primers (see Materials and Methods).

= 1.32) (Konnerth et al., 1987; Bevan and Yeats, 1991); (2) if most capsaicin-sensitive sensory neurons display biphasic pH responses, some display either the fast or the slow component (Krishtal and Pidoplichko, 1981; Bevan and Yeats, 1991); and (3) the two phases appear to be differentially regulated by nerve growth factor in primary cultured sensory neurons (Bevan and Winter, 1995). The ionic selectivity favoring sodium over potassium ions and the low sensitivity to pH of hASIC3 suggest that it is associated with other ASICs or non-ASIC partners in sensory neurons to generate a native heteromeric channel with emergent phenotype not predicted from the properties of each individual component. Indeed, Lingueglia and colleagues (1997) reported that DRASIC could associate with silent MDEG2, a splicing variant of MDEG, to produce a proton sensor poorly sensitive to pH but endowed with a weak cation selectivity closer to the properties of the native current. Alternatively, it is also possible that posttranslational modifications of proton sensor subtypes composed of known subunits could explain the nonselective and sustained ionotropic responses elicited by small pH changes in mammalian sensory neurons.

Acknowledgment: We thank Dr. E. Hamel (Montreal Neurological Institute, McGill University) for the availability of postmortem human trigeminal ganglia. We also gratefully acknowledge the Astra Research Center in Montreal, the Medical Research Council of Canada (MRC), the Savoy Foundation for Epilepsy (SFE), the T2C2 Group, as well as the Fondation des Maladies du Coeur du Québec for their operating support. K.B. is an MRC-Astra postdoctoral Fellow, K.-T.L. holds a PhD studentship from the SFE, and P.S. is a junior Scholar from the Fonds de la Recherche en Santé du Québec.

REFERENCES

Adams C. M., Anderson M. G., Motto D. G., Price M. P., Johnson W. A., and Welsh M. J. (1998) Ripped pocket and pickpocket, novel *Drosophila* DEG/ENaC subunits expressed in early development and in mechanosensory neurons. *J. Cell Biol.* **140,** 143–152.

Bassilana F., Champigny G., Waldmann R., de Weille J. R., Heurteaux C., and Lazdunski M. (1997) The acid-sensitive ionic channel subunit ASIC and the mammalian degenerin MDEG form a heteromultimeric H^+-gated Na^+ channel with novel properties. *J. Biol. Chem.* **272,** 28819–28822.

Bertrand D., Cooper E., Valera S., Rungger D., and Ballivet M. (1991) Electrophysiology of neuronal nicotinic acetylcholine receptors expressed in *Xenopus* oocytes following nuclear injection of genes or cDNAs, in *Methods in Neurosciences* (Conn M. P., ed), pp. 174–193. Academic Press, San Diego.

Bevan S. and Winter J. (1995) Nerve growth factor (NGF) differentially regulates the chemosensitivity of adult rat cultured sensory neurons. *J. Neurosci.* **15,** 4918–4926.

Bevan S. and Yeats J. (1991) Protons activate a cation conductance in a subpopulation of rat dorsal root ganglion neurones. *J. Physiol. (Lond.)* **433,** 145–161.

Canessa C. M., Merillat A. M., and Rossier B. C. (1994*a*) Membrane topology of the epithelial sodium channel in intact cells. *Am. J. Physiol.* **267,** C1682–C1690.

Canessa C. M., Schild L., Buell G., Thorens B., Gautschi I., Horisberger J.-D., and Rossier B. C. (1994*b*) Amiloride-sensitive epithelial Na^+ channel is made of three homologous subunits. *Nature* **367,** 463–467.

Corey D. P. and Garcia-Anoveros J. (1996) Mechanosensation and the DEG/ENaC ion channels. *Science* **273,** 323–324.

Coscoy S., Lingueglia E., Lazdunski M., and Barbry P. (1998) The Phe-Met-Arg-Phe-amide-activated sodium channel is a tetramer. *J. Biol. Chem.* **273,** 8317–8322.

De Léan A., Munson P. J., and Rodbard D. (1978) Simultaneous analysis of families of sigmoidal curves: application to bioassay, radioligand assay, and physiological dose-response curves. *Am. J. Physiol.* **235,** E97–E102.

Dray A. and Perkins M. (1993) Bradykinin and inflammatory pain. *Trends Neurosci.* **16,** 99–104.

Firsov D., Gautschi I., Merillat A.-M., Rossier B. C., and Schild L. (1998) The heterotetrameric architecture of the epithelial sodium channel (ENaC). *EMBO J.* **17,** 344–352.

Garcia-Anoveros J., Derfler B., Neville-Golden J., Hyman B. T., and Corey D. P. (1997) BNaCl and BNaC2 constitute a new family of human neuronal sodium channels related to degenerins and epithelial sodium channels. *Proc. Natl. Acad. Sci. USA* **94,** 1459–1464.

Ishibashi K. and Marumo F. (1998) Molecular cloning of a DEG/ENaC sodium channel from human testis. *Biochem. Biophys. Res. Commun.* **245,** 589–593.

Kleyman T. R. and Cragoe E. J. (1988) Amiloride and its analogs as tools in the study of ion transport. *J. Membr. Biol.* **105,** 1–21.

Konnerth A., Lux H. D., and Morad M. (1987) Proton-induced transformation of calcium channel in chick dorsal root ganglion cells. *J. Physiol. (Lond.)* **386,** 603–633.

Krishtal O. A. and Pidoplichko V. I. (1981) A receptor for protons in the membrane of sensory neurons may participate in nociception. *Neuroscience* **6,** 2599–2601.

Krishtal O. A., Osipchuk Y. V., Shelest T. N., and Smirnoff S. V. (1987) Rapid extracellular pH transients related to synaptic transmission in rat hippocampal slices. *Brain Res.* **436,** 352–356.

Lennon G., Auffray C., Polymeropoulos M., and Soares M. B. (1996) The I.M.A.G.E. consortium; an integrated molecular analysis of genomes and their expression. *Genomics* **33,** 151–152.

Lindahl O. (1974) Pain—a general chemical explanation. *Adv. Neurol.* **4,** 45–47.

Lingueglia E., Champigny G., Lazdunski M., and Barbry P. (1995) Cloning of the amiloride-sensitive FMRFamide peptide-gated sodium channel. *Nature* **378,** 730–733.

Lingueglia E., de Weille J. R., Bassilana F., Heurteaux C., Sakai H., Waldmann R., and Lazdunski M. (1997) A modulatory subunit of acid sensing ion channels in brain and dorsal root ganglion cells. *J. Biol. Chem.* **272,** 29778–29783.

North R. A. (1997) Families of ion channels with two hydrophobic segments. *Curr. Opin. Cell Biol.* **8,** 474–483.

Price M. P., Snyder P. M., and Welsh M. J. (1996) Cloning and expression of a novel human brain Na^+ channel. *J. Biol. Chem.* **271,** 7879–7882.

Snyder P. M., Cheng C., Prince L. S., Rogers J. C., and Welsh M. J. (1998) Electrophysiological and biochemical evidence that DEG/ENaC cation channels are composed of nine subunits. *J. Biol. Chem.* **273,** 681–684.

Tavernarakis N., Shreffler W., Wang S., and Driscoll M. (1997) *unc-8*, a DEG/ENaC family member, encodes a subunit of a candidate mechanically gated channel that modulates *C. elegans* locomotion. *Neuron* **18,** 107–119.

Waldmann R., Champigny G., Voilley N., Lauritzen I., and Lazdunski M. (1996) The mammalian degenerin MDEG, an amiloride-sensitive cation channel activated by mutations causing neurodegeneration in *Caenorhabditis elegans. J. Biol. Chem.* **271,** 10433–10436.

Waldmann R., Bassilana F., de Weille J., Champigny G., Heurteaux C., and Lazdunski M. (1997*a*) Molecular cloning of a non-inactivating proton-gated Na^+ channel specific for sensory neurons. *J. Biol. Chem.* **272,** 20975–20978.

Waldmann R., Champigny G., Bassilana F., Heurteaux C., and Lazdunski M. (1997*b*) A proton-gated cation channel involved in acid-sensing. *Nature* **386,** 173–177.